ENVIRONMENTAL RESEARCH
COMMUNICATIONS

INCLUSIVE PUBLISHING TRUSTED SCIENCE
PURPOSE-LED PUBLISHING™

PAPER • **OPEN ACCESS**

Spatiotemporal variability in global lakes turbidity derived from satellite imageries

To cite this article: Defeng Wu *et al* 2025 *Environ. Res. Commun.* **7** 035007

Environmental Research Communications

PAPER

Spatiotemporal variability in global lakes turbidity derived from satellite imageries

Defeng Wu[1,2,3], **Ting Tang**[4,5], **Daniel Odermatt**[6,7] and **Wenfeng Liu**[1,2,3]

[1] State Key Laboratory of Efficient Utilization of Agricultural Water Resources, China Agricultural University, Beijing 100083, People's Republic of China
[2] National Field Scientific Observation and Research Station on Efficient Water Use of Oasis Agriculture in Wuwei of Gansu Province, Wuwei 733000, People's Republic of China
[3] Center for Agricultural Water Research in China, College of Water Resources and Civil Engineering, China Agricultural University, Beijing 100083, People's Republic of China
[4] Biological and Environmental Science and Engineering Division, King Abdullah University of Science and Technology, Thuwal 23955, Saudi Arabia
[5] Water Security Research Group, Biodiversity and Natural Resources Program, International Institute for Applied Systems Analysis, Schlossplatz 1, A-2361, Laxenburg, Austria
[6] Eawag, Swiss Federal Institute of Aquatic Science and Technology, 8600 Dübendorf, Switzerland
[7] Department of Geography, University of Zurich, Winterthurerstrasse 190, 8057 Zurich, Switzerland

E-mail: wenfeng.liu@cau.edu.cn **and** wenfengliu@vip.sina.com

OPEN ACCESS

RECEIVED
27 November 2024

REVISED
10 February 2025

ACCEPTED FOR PUBLICATION
21 February 2025

PUBLISHED
5 March 2025

Keywords: global assessment, lake turbidity, climate change impact, lake management, temporal variation analysis

Supplementary material for this article is available online

Abstract

Turbidity is a key indicator of water quality and has significant impacts on underwater light availability of lakes. But the spatiotemporal variability of turbidity, which is important for understanding comprehensive changes in the water quality and status of aquatic ecosystems, remains unclear on a global scale. In this study, the spatial distribution pattern, seasonal variability, spatiotemporal variability, and influencing factors of turbidity in 774 lakes worldwide have been investigated using the turbidity product of Copernicus Global Land Service (CGLS) derived from Sentinel-3 OLCI. We found that 63.4% of lakes show low turbidity ($\leqslant$ 5 Nephelometric Turbidity Units). The ranking of turbidity by climate zone is as follows: arid climate $>$ tropical climate $>$ temperate climate $\sim$ polar climate $>$ cold climate. Turbidity decreased significantly in 40% of studied lakes, and increased significantly in 32% lakes. The lake with low turbidity has less seasonal variation, and there is a large seasonal variation in lake turbidity in the tropical and polar climate zones of Northern Hemisphere. Positive covariates to turbidity of global lakes include wind speed of lake, slope, surface runoff, and population in the catchment. Conversely, negative covariates include lake area, volume, discharge, inflow of lake, and GDP. Abundant water volume, favorable flow conditions, and more financial investments in lake management can help to reduce turbidity. These findings highlight the spatiotemporal changes of global lake turbidity and underlying mechanisms in controlling the variability, providing valuable insights for future lake water quality management.

1. Introduction

Climate change has caused a variety of extreme weather events and other climatic phenomena. The global annual mean temperatures from 2015 to 2022 were the eight warmest on record despite the cooling impact of a La Nina event [1]. These changes have led to strong responses in global lake ecosystems [2–4]. For example, a pervasive and rapid warming was observed in global lake summer surface water temperatures [5, 6]; 53% of global lake water storage decreased statistically significantly over the period 1992–2020 [7]; the storage returns of global reservoir decreased except for those in North America, Europe and Siberia during 1999–2018 [8]; and total suspended sediments (TSS) have decreased in most lakes of the Middle and Lower Yangtze River basin over

the period 2000–2014 [9]. Healthy aquatic ecosystems are crucial for sustaining biodiversity of water bodies, safeguarding our drinking water resources, and supporting human well-being [10–12].

Turbidity is a key indicator of water clarity [13, 14], and it is a measurement of diffuse attenuation or side scattering at NIR (Near Infrared) wavelength [15]. Attenuation is the sum of NIR scattering and NIR absorption, reduced underwater light availability at depth, and it is largely a proxy of particle scattering and concentration since NIR absorption of pigments and CDOM is low. Turbidity can be measured by two approaches, nephelometry and turbidimetry, for low and high turbidity levels, respectively [15]. Increasing turbidity reduces water clarity for transmitted light, facilitating the thermal stratification of the lake [16], further altering the lake mixing regime together with the increasing air temperature, and the in-lake biogeochemical process [17, 18]. Therefore, it is of significance to reveal how changes in aquatic ecosystems respond to climate change and the major driving factors.

Turbidity, total suspended matter (TSM), and transparency are closely related water quality properties [9], because all of them are tightly related to the scattering of suspended particles. Accordingly, turbidity is directly correlated with TSM [19–21]. High concentrations of TSM (such as suspended sediment, phytoplankton, allochthonous organic particles (e.g. plant debris)) typically indicates a higher turbidity and lower water transparency [22, 23]. Turbidity can be influenced by natural factors (climate, hydrology, geography, lake specific properties, etc) [17] and human activities (domestic and industrial wastewater discharge, agricultural fertilizer application, land use change, etc) [24–26]. Many studies have shown that the turbidity in shallow lakes is more likely to increase with the increase of lake wind under the process of sediment re-suspension [9, 27, 28]. Previous analyses in China [22, 29, 30], Minnesota of the USA [31], and southern Canada [26] have shown that deeper lakes generally have lower turbidity compared to shallow lakes. However, lake depth and wind can not completely dominate the fate of lake turbidity. For example, the high water clarity of shallow lakes in the Eastern China Plain in summer was highly related to low TSM as the strong precipitation and weak sediment resuspension, while low water clarity of deep lakes in the western China plateau was highly related to chlorophyll-a due to the intense phytoplankton growth under the high temperature in summer [22]. Also, as the decrease in wind speed [14], and long-term increase in vegetation coverage within the catchment, e.g., most lakes in northeast China have exhibited a statistically significant decrease in lake turbidity [32]. Therefore, the response of lake turbidity to natural factors and human activities demonstrates a high degree of regional heterogeneity and complex dynamic mechanisms, and current research on the dynamic patterns of turbidity and influencing factors across global lakes remains relatively limited.

In recent years, Sentinel satellites (such as Sentinel-1, Sentinel-2, and Sentinel-3) [33], MODIS and Landsat satellite data have been widely used for assessments of lake water quality, including Secchi Disk Depth [22, 34, 35], SPM [9, 29, 36], and turbidity [14, 37, 38]. For example, surface water temperature and total phosphorus were found as the important factors in explaining the variability of lake turbidity between 2002 and 2012 in European [37]. The increase in turbidity of Tonle Sap Lake in the lower Mekong River during 2004–2021 was more significantly influenced by human activities [38]. However, these previous studies primarily focused on individual lakes or regional lake, and few studies conducted comprehensive investigation on revealing the spatiotemporal variability of lake turbidity response to climate-geography-hydrology-human interaction influences on a global scale. In this study, we close this research gap and detect the spatiotemporal variability of global lakes from January 2017 to December 2022 by utilizing remotely sensing water turbidity of 774 lakes worldwide from the Copernicus Global Land Service (CGLS), which is based on 300 m resolution Sentinel-3 satellite data and aggregated in 10-day averages. The non-parametric Mann-Kendall [39–41] and Sen's slope [42] analysis methods were used to analyze the spatial distribution pattern, seasonal variability, spatiotemporal variability of turbidity in different types of lakes (natural lakes/reservoirs, deep / shallow lakes, and climate classes), and then correlation analysis and general linear model (GLM) were used to reveal the influencing factors. This study provides important information to understand the dynamics of turbidity of global lakes.

2. Materials and methods

2.1. Data sources and data processing

The Copernicus Global Land Service (CGLS, https://land.copernicus.eu/global/) provides different water quality products for lakes and reservoirs in the whole world. Turbidity is available in 10-day averaged 300 m raster data for the periods between 2002 to 2012, based on Envisat MERIS, and for 2016 to present, based on Sentinel-3 OLCI. The version 1 products of CGLS consist of data for 1015 lakes. The products are processed using the Calimnos processing chain [43]. They are based on a combination of algorithms for TSM retrieval [44–46] which apply suitable spectral bands for a priori estimated optical water types [47]. The TSM estimates obtained in such manner are then converted to turbidity (conversion factor of 1.17 NTU/g m^{-3} as formulated by [19, 20]).

The water quality data derived from Envisat MERIS (2002–2012) of CGLS have been extensively used in previous studies and showed reliability [37, 38, 48, 49]. These analyses derived from the CGLS have shown that the *Calimnos* processing chain can be applied to both sensors, Envisat MERIS (2002–2012), and Sentinel-3 OLCI (2016-present) [50]. The further optimized *Calimnos* v2 was applied to Sentinel-3 OLCI (2016 - present), and a new Lake Ice Cover algorithm was used to get more accurate ice masking and water surface [50]. The validation results (9 lakes were included) in the CGLS quality assessment report [51] show the lake water turbidity derived from Sentinel-3 OLCI (2016 - present) performed well, and consistency between Sentinel-3 OLCI turbidity and observations is high between years (2016–2019), indicating the suitability of the Sentinel-3 OLCI for detecting spatiotemporal changes of turbidity. We also performed cross validation with remote-sensed Forel-Ule Index (FUI) [52], highly related to turbidity [30]. The results showed that the R of linear regression model between FUI and turbidity in 41.1% available lakes was $\geqslant 0.45$ (99/241 lakes), the R in 36.1% lakes was $\geqslant 0.5$, and the R in 14.1% lakes was $\geqslant 0.7$ (figures S1, S2, and table S1). This cross validation further confirms the reliability of the turbidity data.

In this study, lake-wise spatial aggregation of the 10-day raster data was carried out with the same Python scripts used by [48]. It iteratively runs the operator *StatsOp* in ESA's SNAP toolbox [53] for the lake shapefiles provided by CGLS, and extracts the spatial median value from the CGLS turbidity raster data for all analysis in this study. Of the 1,015 lakes, we excluded 271 lakes which have no data for more than 30% of the time series, and time points were filtered out if less than 50% of the lake's surface was visible for any given 10-day period. For the data gaps resulting from ice or cloud coverage, we fill in the data gaps in the time series using a bootstrapping approach inside a 1-year-long moving window centered around the date of interest [48]. Finally, the monthly turbidity time series of 774 lakes, from January 2017 to December 2022, were used in this study.

Raster data of potential covariates (see table S2) were extracted in a similar manner. In extracting the spatial average value of covariates in the lake catchment, we prepared the drainage catchments of lakes using the HydroATLAS dataset [54, 55] and lake boundaries from CGLS. The HydroLAKES database [56] was used to verify and correct some erroneous CGLS polygons. The covariates considered in this study include: lake attributes (geographical coordinates, lake area, lake depth, slope, lake type, etc) from the HydroLAKES, meteorological data (temperature, precipitation, surface runoff, wind speed, etc) from the ERA5-land dataset [57], the global population from the Gridded Population of the World (GPW) version 4 [58], gross domestic product (GDP) from the Gridded global datasets for Gross Domestic Product [59]. Furthermore, the Köppen-Geiger climate classification [60] was used. A full description and data sources of the covariates are described in table S2 section of Supplementary Information.

According to the guidelines for drinking water quality of the World Health Organization (WHO), the water turbidity should be below 1 NTU for drinking purpose and not exceed 5 NTU for other consumption purposes [23]. The average turbidity of global 774 lakes between January 2017 and December 2022 was divided into two groups (low turbidity: $\leqslant 5$ NTU, and high turbidity: > 5 NTU). Meanwhile, considering that a large number of lakes in Canada in this study (with low values) and water quality guidelines for the protection of aquatic life based on Canadian council of ministers of the environment (CCME), lake average turbidity in figure S1 was further divided into 6 categories (0∼1, 1∼2, 2∼5, 5∼10, 10∼15, >15 NTU). Furthermore, lake types (natural lake or reservoir) were reported as important influencing factors for lake water storage [7]. Turbidity differences between natural lakes and reservoirs, as well as between deep and shallow lakes [22, 29, 30] were also analyzed. The sources of guidelines are described in the Methods section of Supplementary Information.

2.2. Time series analysis

To eliminate the impact of monthly seasonal cycles on all the variables (turbidity and other covariates), the seasonal-trend decomposition procedure based on Loess (STL) method was used. This method, widely used in the time-related data analysis [61, 62], can decompose time series into three component sub-series: seasonal, trend, and residual:

$$Y_t = T_t + S_t + R_t \tag{1}$$

where Y_t is the observed value at the date t; T_t is the trend component (hereafter referred to as TC-STL); S_t is the seasonal component; R_t is the residual component which represents the remaining variation beyond seasonal and trend components. Therefore, the time series in this study includes the raw time series of turbidity, and the TC-STL of all variables.

Afterwards, Sen's slope analysis method [42] was used to estimate the change in slope of the time series (TC-STL and raw time series). The Z statistics from non-parametric Mann-Kendall (hereafter referred to as M-K test) were used to detect the significance of changes of the time series. There is no statistically significant change in variable time series when the $|Z| \leqslant 1.96$ (significance level $\alpha = 0.05$); otherwise, the change in variable time series is statistically significant at significance levels. Negative values of Z indicate decreasing trends in variable time series, whereas positive value indicates upward trends.

2.3. Statistical analysis

For the analysis of lake turbidity with reference to lake types and proprieties, climate regions, and social perspectives, we used correlation analysis and multiple general linear model (GLM). We calculated the Pearson correlation coefficient to identify the linear relationships between Z value of turbidity obtained from M-K test and various covariates considering different lake conditions. The p-value (2-tailed significance test) and Pearson correlation coefficient for each covariate were also used to indicate the strength and direction (positive or negative) of the relationship. The influence of the covariate on Z value of turbidity is statistically significant when p-value of the Pearson correlation coefficient is less than 0.05.

The possible covariates and drivers of lake turbidity include precipitation, temperature, runoff, wind speed, lake water storage, lake depth, and anthropogenic activities, etc. Referring to the statistical analysis of Gilarranz *et al* (2022) [48], we chose GLM, which was commonly used in studying the driving factors of water quality [29, 63, 64], and used the binary values (1 or 0) for the response variables to analyze the variability of global lake turbidity. Before using the GLM, all explanatory variables were scaled, and were log-transformed when necessary to normalize the data. This process helps deal with the nonlinear effect [65]. Three GLMs, considering a binomial distribution, were applied to assess the relationship between these covariates and drivers, and the temporal variation of turbidity. In the three GLMs, the response variable was set to either 1 (significant increase in lake turbidity) or 0 (significant decrease) in GLM 1; the response variable was either 1 (significant increase in lake turbidity) or 0 (nonsignificant increase) in GLM 2; and the response variable was either 1 (significant decrease in lake turbidity) or 0 (nonsignificant decrease) in GLM 3. Through these three models, we can determine the contribution and direction of each driving factor to the lake turbidity under the scenarios of significant increase/decrease (GLM 1), significant/non-significant increase (GLM 2), and significant/non-significant decrease (GLM 3). We conducted variable selection that when the correlation coefficient between the original explanatory variables is greater than 0.5, one of the two is deleted to avoid the strong multicollinearity [66], and the remaining variables were scaled so that the effect sizes are comparable. The final selected models were fitted to the data by maximizing log-likelihood. The final used variables are shown in SI appendix. All the analyses were performed with R 4.1.2. It should be noted that turbidity and other variables in these statistical analyses used the TC-STL of these variables.

3. Results

3.1. Spatial difference of average turbidity in global lakes

We found that the average turbidity in 63.4% of the studied lakes was below 5 NTU over the period January 2017 and December 2022 (figure 1), which is suitable for diverse consumption regarding the lake turbidity requirements of WHO [23]. Lake turbidity below 1 NTU (drinking water requirements) was observed in only 7.5% of the studied lakes, and almost all of which are deep and large lakes (figures S3, S4). Figure S5 shows the spatial distribution of lake area (a) and water depth (b) of 774 lakes worldwide. Specially, two-thirds (63.4%) of lakes with low turbidity ($\leqslant$ 5 NTU) are deep lake (average lake depth greater than 10 m), while more than 70% of lakes with high turbidity ($>$ 5 NTU) are shallow lakes. Turbidity in shallow lakes is significantly higher than that of deep lakes, which have lower variabilities in deep lakes (figure 1(e)). Interestingly, statistically significant differences in turbidity were found between natural lakes with different water depths and lake sizes, but were not observed in different reservoirs (figure S6). The turbidity in deep natural lakes is significantly lower than that of all reservoirs, while the turbidity in shallow natural lakes is the opposite. In addition, the turbidity in small natural lakes is significantly higher than that of large natural lakes and reservoirs (figures S4, S6), while the difference with that of small reservoirs is not significant. The condition of large natural lakes is also the opposite. The lake turbidity in arid climate (the Köppen-Geiger B climate classification) is significantly higher than that of others, while lakes of cold climate (D) had significantly lower turbidity as well as lower variability. The ranking of turbidity by climate zone is as follows: B (arid climate) $>$ A (tropical climate) $>$ C (temperate climate) $\sim$ E (polar climate) $>$ D (cold climate). Spatially, lakes in North America, Europe, and Tibetan Plateau are dominated by low turbidity, while African lakes are dominated by high turbidity ($>$ 15 NTU, figure S3), although some low turbidity levels in lakes are observed in the west branch of Rift Valley in Africa. Furthermore, we found that lakes over Bolivia, Kazakhstan, and the eastern China had predominantly medium turbidity (5 $\sim$ 15 NTU, figure S3).

3.2. Seasonal variability in global lake turbidity

We found that the seasonal variation of lake turbidity in E climate zone of the Northern Hemisphere is the largest, followed by the A climate zone and the C climate zone of Northern Hemisphere (figure 2). In terms of continents, lakes with low multi-year average turbidity have small seasonal variations (figure S7), such as North America, Europe, and Southeast Asia, while lakes with high multi-year average turbidity have large seasonal

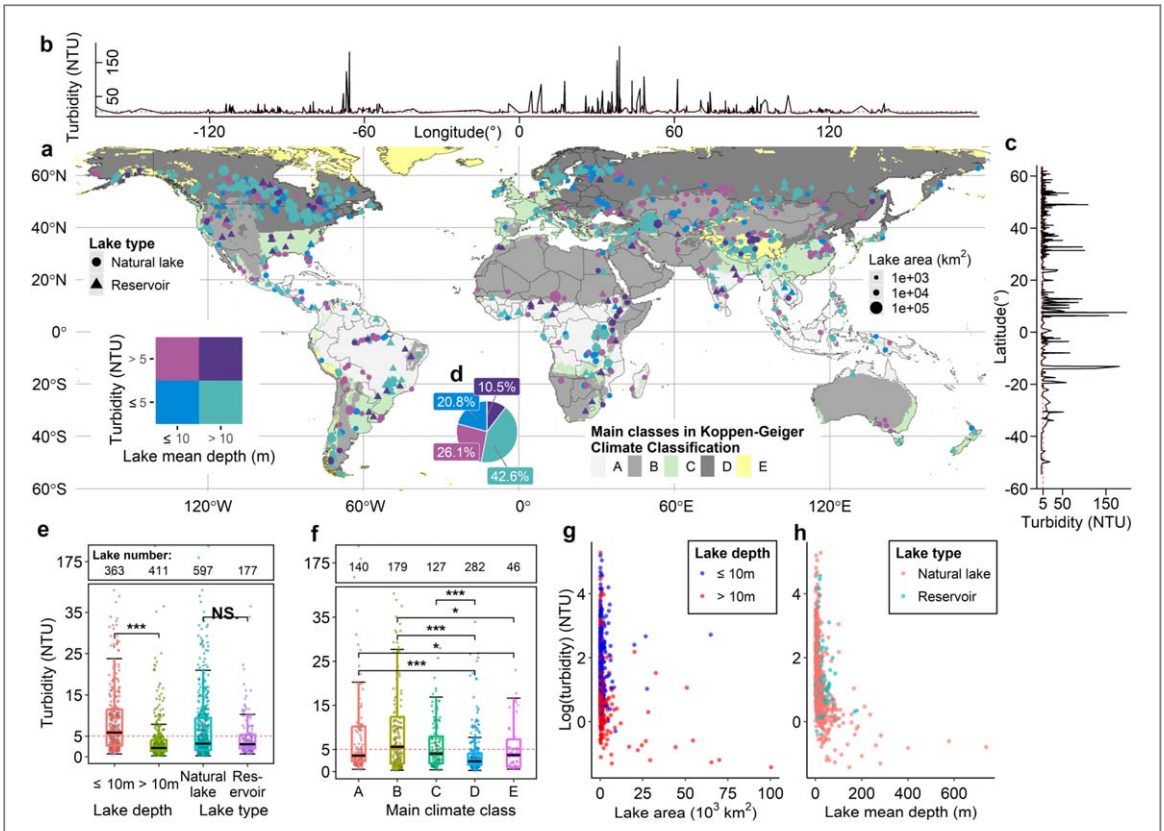

Figure 1. Global patterns of turbidity in 774 lakes (natural lake and reservoir) between January 2017 and December 2022. (a). The spatial distribution of monthly average turbidity, lakes are colored by two turbidity levels (low turbidity: $\leqslant 5$ NTU, high turbidity: > 5 NTU) and two lake depth types (shallow lakes: $\leqslant 10$ m, deep lakes: > 10 m). Each point represents one center of the 774 lakes. Colors of land illustrate the dominant climate classes in Köppen-Geiger climate classification [60] (tropical climate (A), arid climate (B), temperate climate (C), cold climate (D), polar climate (E)). b ~ c: Lake average turbidity across different longitudes and latitudes are summarized. d: The percentage of specific-colored lakes in total lakes studied. e ~ f: The differences of lake turbidity across different lake depth, lake type (natural lake or reservoir), and the Köppen-Geiger climate classification. 2-sample test (wilcox.test) was used for data comparison, illustrating with several degrees of statistical significance (NS: $p > 0.05$, *: $p < 0.05$, **: $p < 0.01$, ***: $p < 0.001$). g ~ h: The nonlinear relationship between log-transformed lake turbidity, lake area (g), and lake mean depth (h). The colors of data points correspond to the different lake depth (g), and lake type (h). The figure was created using R 4.1.2.

variations, such as West Africa, East Africa, and Central Asia. In addition, the seasonal variation of lake turbidity in South Asia is very significant, followed by lakes in South America and East Asia.

We further mapped the seasonal turbidity distribution of global lakes over 2017 to 2022 (figure S8), and compared the seasonal changes of lake turbidity in different years (figure S9). Similar to the results of the box plot (figure S7), we found that there was no obvious seasonal change in lakes in North America and Europe. Compared with spring (figure S9), the turbidity of lakes, in Africa, South America and India, increased significantly in summer, and decreased significantly in winter. Differently, the turbidity of lakes in the Tibet Plateau decreased significantly in autumn, while increased significantly in winter. Meanwhile, an interannual variation in lake turbidity in different seasons also was observed (figure S10). Compared with the turbidity in 2017, we found that, most lakes in North America and Northern Europe showed a significant increase of turbidity in the spring, summer, and winter of 2018–2019. Also, the spring turbidity of lakes in the Tibet Plateau increased significantly since 2020, while the winter turbidity increased since 2017. The turbidity of lakes in all seasons in African and Oceania, generally decreased year by year since 2017. The summer turbidity of lakes in the Amazon River Basin increased significantly in 2020 and 2022. The summer turbidity of lakes in Indian increased since 2017, the autumn turbidity increased significantly in 2019, and the winter lakes decreased since 2017. The turbidity of lakes in eastern China, in summer and autumn, generally increased in 2021–2022.

3.3. Spatiotemporal variability in global lake turbidity

Based on the raw monthly turbidity data, 198 lakes show a statistically significant decrease, and 163 lakes show a statistically significant increase for the period of January 2017 to December 2022 (figure S11(a)). However, from the results of the M-K test, we found that removing monthly seasonal cycles from raw time series of lake turbidity using STL helps identify more accurate changes, as has been reported in other studies [67, 68]. After the seasonal cycle was removed, we found that 310 lakes show a statistically significant decrease between 2017 to

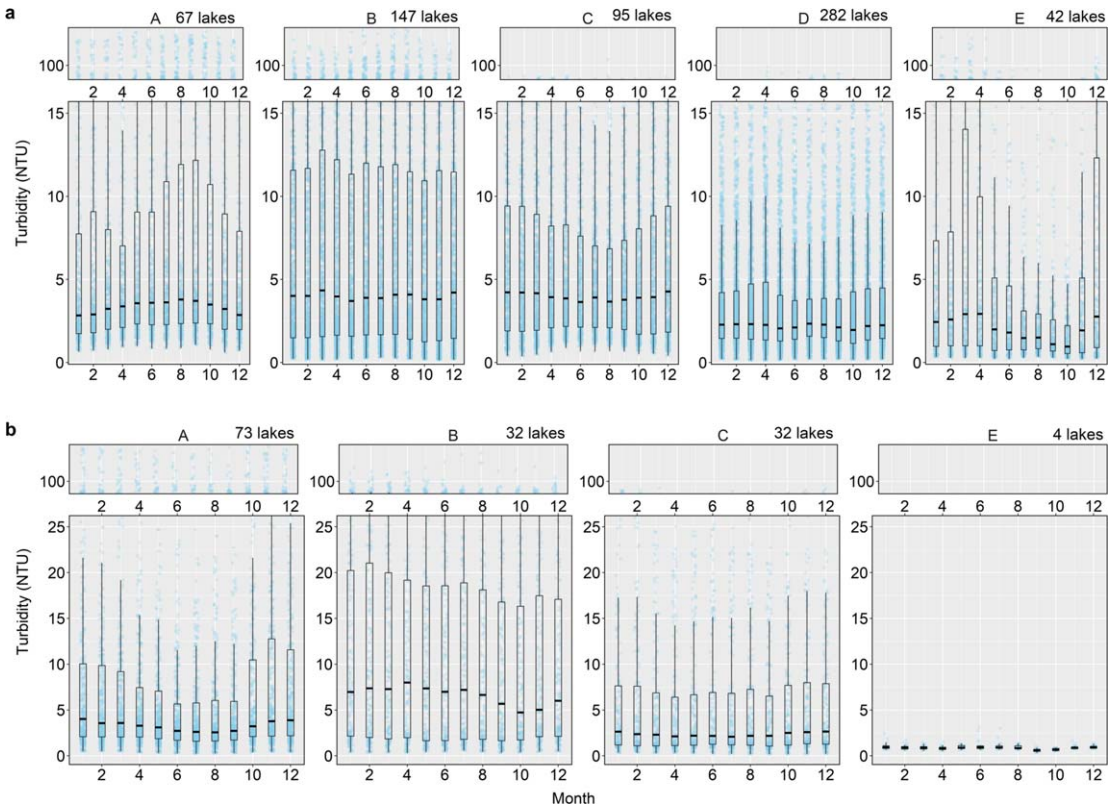

Figure 2. Seasonal variability of monthly turbidity among different climate classes in global 774 lakes (Northern hemisphere (a), and Southern Hemisphere (b)). Northern Hemisphere: March to May is spring, June to August is summer, September to November is autumn, December to February is winter; Southern Hemisphere: March to May is autumn, June to August is winter, September to November is spring, December to February is summer.

2022, and 248 lakes show a statistically significant increase (figure 3). The results confirm that the removal of seasonal cycle strengthens the identification of temporal variation. There is a higher probability of misjudgment in the M-K test including seasonal cycles when the change rate in lake turbidity is small, e.g., for the change rate ranges from −0.01 to 0.01 (figures S11(c) ∼ (d)). Especially, the M-K test with seasonal cycles exhibited the highest rate of misjudgment in lake turbidity in the United States (31/78 lakes) (figures S11(a) ∼ (b)). Therefore, this study mainly analyzes the temporal variation of lake turbidity without monthly seasonal cycle, that is, the change rate of TC-STL of lake turbidity.

The lakes in Northeast America and East Africa are clustered with a significant decrease in lake turbidity (figure 3). For specific countries, Canada has the highest number of lakes with a significant decrease in turbidity (65/150 lakes) in the world, while China has the highest number of lakes with a significant increase in turbidity of our studied lakes (46/111 lakes). Furthermore, particular concerns are the hotspots with medium and high average turbidity, such as Bolivia, Kazakhstan, and eastern China, which also show a significant increase in turbidity (figures 1, 3, S12). There are significant differences for lake turbidity changes in different climate regions, especially the cold climate (D), tropical climate (A), and polar climate (E) (figure 3(d)). As shown by figures S13 and 3(c), significant increases in turbidity are observed in lakes with low average turbidity (2 ∼ 5 NTU) in tropical climate, while decrease in turbidity are observed in some lakes with high average turbidity (> 5 NTU). Meanwhile, significant decreases in turbidity are observed in most lakes in cold climate except for the lakes with super high average turbidity (> 15 NTU), and significant increases in lake turbidity are observed in most lakes in polar climate except for several lakes with low average turbidity (⩽ 2 NTU). As shown in figure S14, nearly all the studied lakes in polar climate are located on the Tibetan plateau. Unlike the average turbidity of global lakes, which is mainly affected by lake depths, the temporal variation of global lakes is mainly affected by lake sizes. As shown in figures S15 and S16, we found that the turbidity in large lakes decreased significantly, while the turbidity in small lakes increased significantly. No significant difference was observed between the turbidity changes of lakes with different depths, but there was a strong significant difference between the significant decrease in turbidity in shallow large lakes and the turbidity changes in deep small lakes.

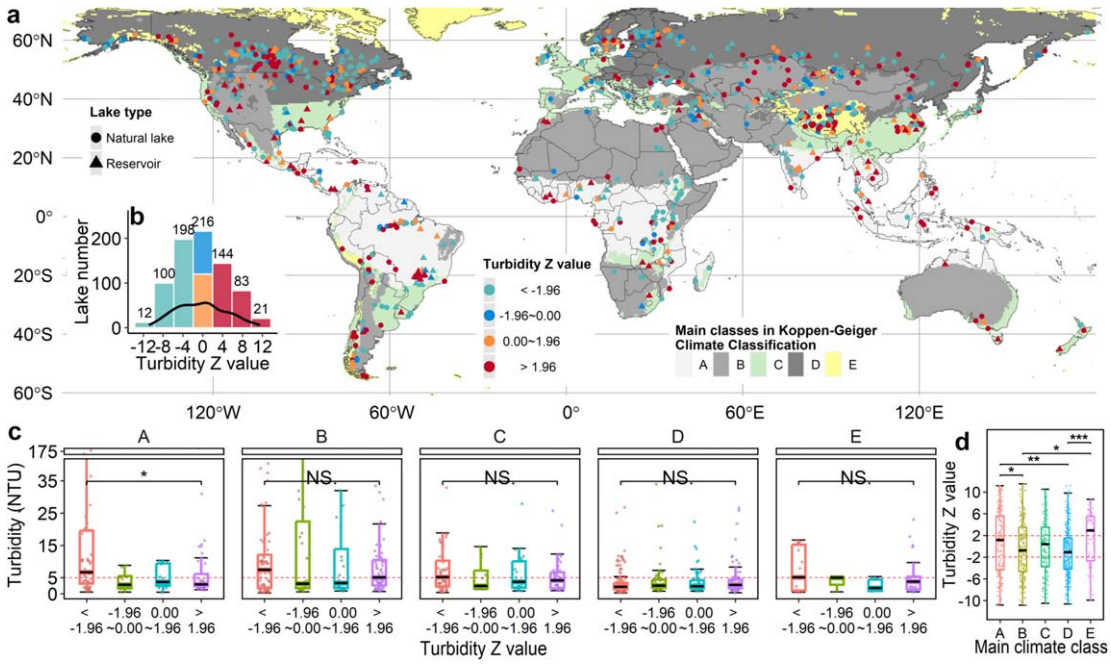

Figure 3. Results of M-K test in lake turbidity time series. a: The spatial distribution of Z value of lake turbidity. Significant decreases in lake turbidity are shown in light blue (40.1% of 774 lakes), while non-significant decreases are shown in blue (12.4%). Non-significant increases in lake turbidity are shown in orange (15.5%), while significant increases are red (32%). The inserted subplot b shows the histogram of lakes with four types of turbidity changes. Here, turbidity refer to the TC-STL of lake turbidity. Z values of lake turbidity are estimated by the M-K test, and constructed on a critical value of ± 1.96 ($p < 0.05$). c: The differences of lake turbidity (average turbidity) across four types of turbidity changes. d: The differences of Z value of lake turbidity across main Köppen-Geiger climate classification. The test method in boxplots for data comparison and the symbols indicating statistical significance are same as figure 1. The meaning of the points and the colors of the land on the map are the same as in figure 1.

3.4. Relationships between lake turbidity changes and other factors

Figure 4 features the bivariate maps based on the Z values of the M-K test for turbidity, precipitation, and air temperature over the period between Januar0y 2017 and December 2022. These maps indicate that the lakes, around the Great Lakes and the reservoirs in eastern Canada, show a significant increase in air temperature with significantly decreasing precipitation and turbidity figure S17). Other hotspots are the Nile basin and the east branch of the Rift Valley in Africa with significant decreasing of precipitation, temperature and turbidity. Furthermore, particular concern hotspots with relatively high turbidity and significant increases in lake turbidity, such as Bolivia and Kazakhstan, presented a significant increase in temperature and significant decrease in precipitation.

We further combined the results of correlation analysis and GLMs to examine the relationship between lake turbidity changes and other factors (table S3 and figure 5). In addition to latitude, the other significant factors can be broadly grouped into three categories: hydroclimatic factors (temperature, runoff, and wind speed), catchment and lake properties (slope of catchment, lake area and inflow), and socio-economic factors (population and GDP). A robust and significant negative relationship is observed between latitudes and Z value of turbidity in GLM 1 and GLM 2 (figure 5). This indicates that the higher latitudes of lakes decreased the probability of a lake experiencing a significant increase in turbidity. Meanwhile, the results of the correlation analysis also show the same relationship (table S3).

For hydroclimatic factors, the Z values of wind speed in GLM 1 has a statistically significant positive effect on lake turbidity, indicating that wind speed in the catchment increases the probability of a lake experiencing a significant increase in turbidity. Similar condition is also observed in the shallow natural lakes of the correlation analysis results (table S3). In addition, a significant and negative relationship between temperature and Z value of turbidity (figure 5) may suggest that the turbidity of lakes with higher monthly mean temperature is more likely to decrease significantly, while that of lakes with lower monthly mean temperature is more likely to increase significantly, except for the global shallow reservoirs (table S3). This may be due to the significant increase of turbidity in many lakes located in the cold region (Central Canada and the E climate zone), and the significant decrease of lake turbidity in the African Rift Valley (hot region) (figures 3, S18). However, there is a robust positive influence on the increase of lake turbidity from surface runoff in the catchment, while total runoff presents a robust negative influence on increasing lake turbidity (figure 5).

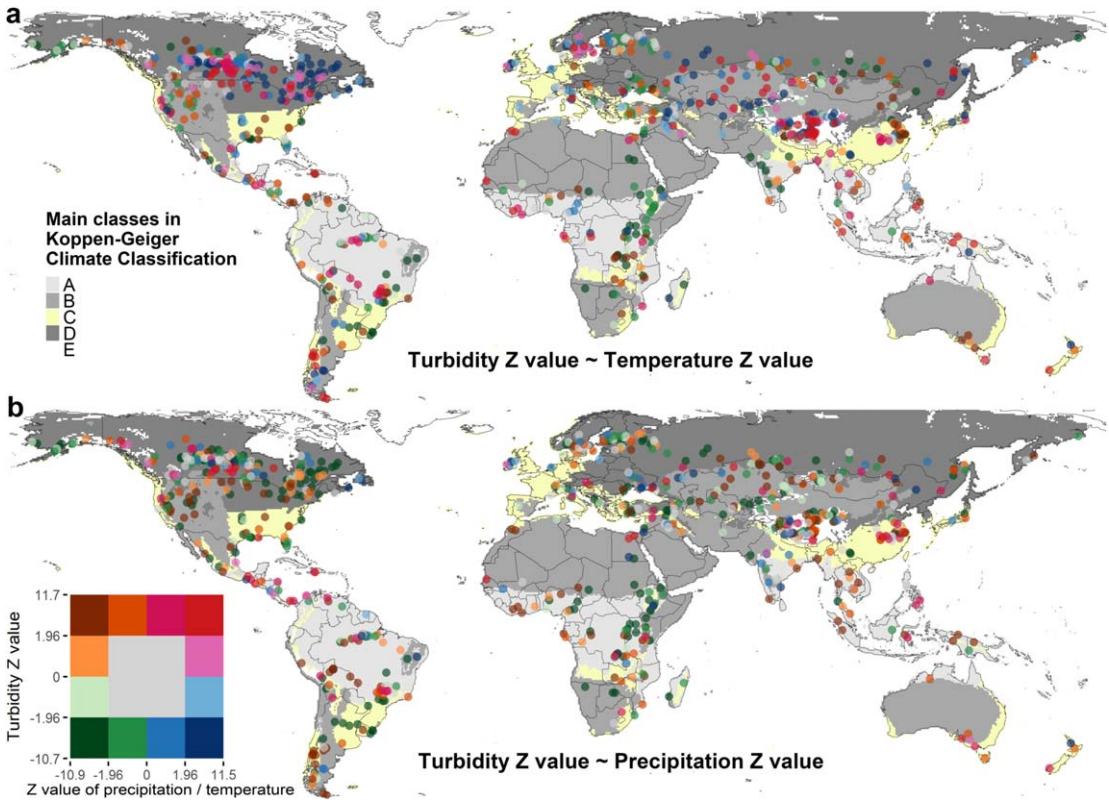

Figure 4. 4 × 4 tile bivariate maps of Z values of (a) between air temperature and turbidity, and (b) between precipitation and turbidity. Turbidity, precipitation, and air temperature refer to their respective TC-STL time series. Z values of turbidity, precipitation, and air temperature are estimated by the M-K test. Z values for all variable are constructed on a critical value of ±1.96 ($p < 0.05$). Other maps of the Z values of precipitation and temperature are shown in figure S17. Colors of land illustrate the dominant climate classes in Köppen-Geiger climate classification.

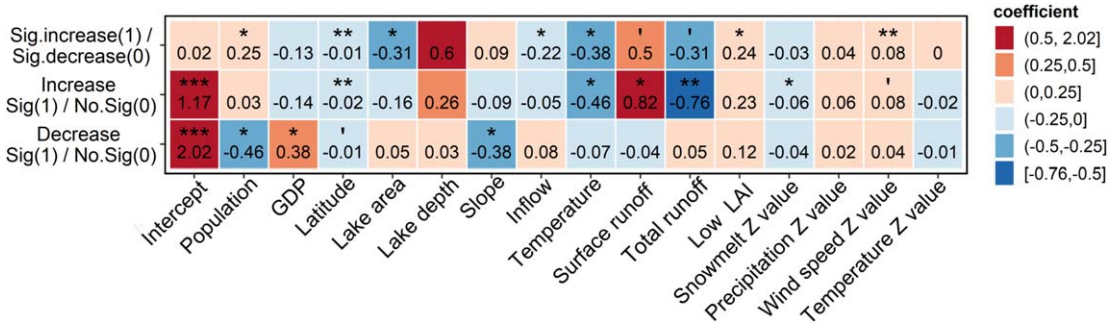

Figure 5. Factors affecting the turbidity change based on the multiple general linear models. These are three multiple general linear models (GLM) using a binomial distribution. The response variable is either 1 (significant increase in turbidity) or 0 (significant decrease) in GLM 1; the response variable is either 1 (significant increase in turbidity) or 0 (nonsignificant increase) in GLM 2; and the response variable is either 1 (significant decrease in turbidity) or 0 (nonsignificant decrease) in GLM 3. Red factors represent positive effects, while blue factors represent negative effects. Effect significance factor is denoted by an asterisk, where ' means $p < 0.1$, * $p < 0.05$, ** $p < 0.01$, and *** $p < 0.001$. In particular, after the non-significant variables were deleted one by one, except for temperature and low vegetation LAI in GLM 1, other significant variables were still significant in the final models. Z values of all variable are estimated by the M-K test, and constructed on a critical value of ±1.96 ($p < 0.05$). More detailed meanings of factors, used in GLM and figure 5, are given in table S2.

The catchment and lake properties, such as water storage volume, lake inflow, lake discharge, catchment area, and lake area have a consistent and significant positive effect on the decrease in turbidity (table S3). To be clear here that the correlation between lake area and catchment area is extremely high (Pearson correlation coefficient > 0.6). On the contrary, a robust positive influence on the increase of lake turbidity from the average slope within 100 m around the lake was observed as well.

For the socio-economic drivers, population density within the catchment is significantly positively correlated to lake turbidity, while the average GDP in the catchment has a significant effect on decreased that

probability. In other words, wealthier areas tend to have a higher probability of significant decreases in lake turbidity, possibly due to more effective water environmental management strategies to improve water quality [48].

In addition, we further conducted Pearson correlation analysis between lake turbidity and factors in different climate classes (table S4). We first found some similar relationship to the results of GLM on global lakes. For example, we found that the catchment and lake properties, such as water volume, and lake area, have a consistent positive effect on the decrease in turbidity in the lakes of different climate classes, and lake depth (table S4). In terms of runoff, the relationship between total runoff and deep lake turbidity in D climate class, surface runoff and shallow lake turbidity in D climate class and lake turbidity in basin 161 in E climate zone is consistent with GLM. Also, the relationship between GDP and deep lake turbidity in C climate class, vegetation index and all lake turbidity in A climate class, total lake wind speed and shallow lake turbidity in D climate class is consistent with GLM.

However, the relationship between lake turbidity and precipitation and temperature is different among different climate classes. For example, a strong positive correlation between temperature and the turbidity of deep lakes in A climate class, while a negative correlation between temperature and the turbidity of all lakes in C climate class and deep lakes in D climate class. A positive correlation between precipitation and turbidity of shallow lakes in C climate class, but a strong negative correlation between precipitation and turbidity of deep lakes in D climate class. Meanwhile, we also found that the relationship between lake turbidity and horizontal wind speed and vertical wind speed is different among different climate classes. GDP has a positive effect on turbidity of deep lakes in A climate class. Besides, there is a significant positive correlation between trophic and turbidity of all lakes in D climate class.

4. Discussion

Our study, for the first time, provides a comprehensive assessment of the spatiotemporal variability in lake turbidity on a global scale. Our findings on lake turbidity with different depths are consistent with previous studies [26, 30, 31] that the average turbidity in global shallow lakes is significantly higher than that of deep lakes, mainly due to the wind and sediment resuspension [9, 27, 28]. We found the turbidity of deep natural lakes is significantly lower than that of all reservoirs, while the opposite is true for shallow natural lakes. The widespread low average turbidity was found for more than 60% lakes, and most of them are located in North America, Tibetan Plateau, and Europe [30]. The low average lake turbidity in the first two regions may be explained by the increased water depth result from the historical increased water storage [22, 69, 70].

By mapping the Z values of turbidity in global lakes from 2017 to 2022, we found a significant latitudinal difference in turbidity of global lakes (figures 3, 5, and table S3), which is most likely caused by hydroclimatic drivers as the opposite changes in lake turbidity between tropical climate, polar climate, and cold climate (figure 3(d)). The same phenomenon has also been observed in studies about water clarity [34]. Our findings suggest that the variability in lake turbidity observed in cold climate zones (D) is significantly likely related to the widespread warming (figures 4, S15), increased wind speed, decreased precipitation, and decreased total runoff in the region (figure S19) [71, 72]. On the other hand, the observed increase of lake turbidity in tropical climate (A) is correlated to increased temperature and phytoplankton growth, and most of them had positive correlations with temperature and LAI (table S4). Previous studies indicate that, as the global warming, the intensity of algal blooms is increasing rapidly in Africa [22, 73], and the proportion of algal bloom outbreaks in tropical lakes is the highest in the past 20 years [70]. Moreover, high precipitation and decomposition of large amounts of organic litter in tropical rainforests [74] may lead to increased turbidity in lakes due to the runoff [75].

One major difference from the results of other studies [22, 29, 30, 34] is that the turbidity of lakes in the Tibet Plateau in this study is rising. The discrepancies may be due to the different lakes studied and the different time periods between previous studies and this study. We found that the seasonal and temporal variation was very similar based comparison of the lake turbidity of CGLS in Tibet Plateau with the FUI in Wang *et al* (2021) [52] during 2016–2018 (figure S2). Also, the seasonal variation (figures S2, S9) was similar with the study of Mi *et al* (2019) [76]. The observed increase of lake turbidity had positive correlations with vertical wind speed, average turbidity and Z value of total runoff of catchment (table S4). Lakes, in Tibet Plateau and polar climate (E), greatly affected by sediments brought by glacial meltwater, have seen a significant increase in lake turbidity, specially in winter and spring (figure S10), due to increased temperature, glacier meltwater, runoff, and sediment during the hottest eight years (https://wmo.int/news/media-centre/eight-warmest-years-record-witness-upsurge-climate-change-impacts) from 2017 to 2022. It was indicated that sediments carried by meltwater would increase the lake turbidity in Tibet Plateau, such as the Lake Silingco [76]. Also, lake warmer, which favors

phytoplankton growth, may be another primary factor controlling the increase of turbidity for lakes, which has been identified in plateau of western China [22, 73].

Furthermore, our study finds that the increase in lake turbidity is significantly likely related to slope and surface runoff. The catchment with higher slope and stronger surface runoff intensity will cause stronger soil erosion and more suspended matter, resulting in an increase in lake turbidity [77, 78]. The slope and surface runoff in the catchment increased the probability of a lake experiencing an increase in lake turbidity, while lake area, flow condition (discharge, inflow, total runoff), water storage of lake largely significantly decreased that probability. This finding is also consistent with the results of study in Canada [26], China [29], and Lake Toshka in Egypt [79]. The significant decrease in turbidity in many lakes over the east branch of Rift Valley in Africa, with the relatively small lake area, large lake depth and high average turbidity ($>$ 15 NTU, figure S3), is primarily attributed to the increase in water storage [69, 70] and the high total runoff (figure S19). The dilution effect from large total runoff on lake turbidity is obvious at the global scale.

For the socio-economic drivers, our findings indicates that the increases in lake turbidity will become more common as the increasing population in the catchment, but are expected to decrease significantly as increase in per capita GDP [48]. This may be because of the improvement of water quality after water environment treatment with high investment, such as Lake Apopka in US (https://lake.wateratlas.usf.edu/waterbodies/lakes/7800/) [80], Lake Dianchi and Lake Tai in China [29]. However, we also found that the influence of GDP on lake turbidity in A climate class is positive (table S4). This may be caused by the imbalance between economic development and environmental protection in underdeveloped areas, as demonstrated in the environmental Kuznets curve (EKC) theory [81, 82]. In contrast to previous findings [22, 29], our findings suggest that increases in lake turbidity in China are more extensive over the period (2017–2022), although we confirm there is a significant decrease in lake turbidity in several lakes with severe eutrophication, such as Lake Dianchi and Lake Tai. This contrast indicates that the difference in results is most likely due to the different study periods [7] and the extreme heat in China in 2022 [83].

This global-scale attribution of lake turbidity change has important implications for water resources management, water security, and other benefits for humanity and ecosystems. Particularly, it is necessary to focus on the lakes with relatively high average turbidity and significant increasing turbidity such as those in Bolivia, Kazakhstan, and eastern China. In Kazakhstan, where the GDP is relatively low compared with the developed countries, there is a significant increase in temperature and a significant decrease in precipitation, probably leading to an increase in lake turbidity in the future. The issue about water resources management in Central Asian countries is multifaceted, complex, and closely related to agricultural activities. To restore and maintain healthy water environments for lakes will require prolonged and comprehensive strategies [84]. Moreover, despite the relatively higher GDP in eastern China, stronger lake management efforts still are necessary in the future to maintain ecosystem health [35] due to the region's large population density and extensive pollutant retention in lakes.

This research reveals the spatial distribution of average monthly turbidity in global lakes, analyzes the seasonal variability, and spatiotemporal variability of lakes turbidity, and highlights the relationship between variability of lakes turbidity and other factors, such as hydroclimatic conditions, catchment characteristics, lake properties, and socio-economic factors. Although there are some limitations in the study, especially length of the time series, satellite observations provide near real-time, high-resolution data for monitoring the lake turbidity on a global scale. Another limitation is related to lake water boundaries (maximum water extent observed), the identification of shallow water areas, and lake ice detection in CGLS. For the lake turbidity in CGLS before 2020, we found that many pixels near the lake boundaries showed extremely large values during the freezing period. This may be because lake turbidity in CGLS in the period 2016–2019 generated using *Calimnos* processing chain v1.3.0 applied a static, incomplete, ice mask, and ice masking performed nominally [43]. But lake turbidity in CGLS after 2020 was produced by *Calimnos* processing chain v1.4.0, which differs from v1.3.0 with improved lake ice detection. Therefore, in this study, lake turbidity when the visibility of the lake surface was less than 50% of lake water boundaries due to lake ice or cloud cover were deleted during data preprocessing to reduce data errors caused by the above limitation. Overall, our results highlight the importance of different factors and underlying mechanisms in the spatiotemporal variability of global lake turbidity, providing valuable insights for future lake water quality management. Future studies should combine more field monitoring data and used nonlinear regression, such as Random Forest, to improve the ability of understanding the causality between lake turbidity and different factors.

5. Conclusion

We analyzed the spatiotemporal patterns of turbidity in 774 large lakes in the world. The average turbidity in 63.4% of the studied lakes was below 5 NTU. The ranking of turbidity by climate zone is as follows: B $>$ A $>$ C $\sim$

E > D. For natural lakes, the turbidity in shallow (small) lakes is significantly higher than that of deep (large) lakes. There is a large seasonal variation in lake turbidity in the E & A climate zone in Northern Hemisphere. While the lakes with low turbidity have less seasonal variation, such as North America, and Europe. The turbidity decreased significantly in 40% of studied lakes, and increased significantly in 32% lakes. The key factors, with a positive correlation to turbidity, include slope, surface runoff, wind speed, and population, while a negative correlation is observed between turbidity and lake area, volume, flow conditions, and GDP. However, the effects of some specific factors, such as precipitation, temperature, and GDP, are different for the turbidity in different classes of lakes. This study suggests the important potential processes for spatiotemporal variability in global lakes turbidity include hydrological process, soil erosion, sediment transport and re-suspension process. High water level, good flow conditions, and more financial investments in lake management can help to reduce lake turbidity.

Acknowledgments

We are grateful to Dr Yuanyuan Huang from Institute of Geographic Sciences and Natural Researouces Resarch of CAS for comments on the methods and writing. This study was supported by the National Natural Science Foundation of China (32361143871, 52109071, 52311540127, and 52411540183) and the Pinduoduo-China Agricultural University Research Fund (Grant No PC2023A02002).

Data availability statement

The data in this paper will also be used by the authors for auxiliary analysis of other studies. Therefore, before the results of other studies are published, the data in this paper cannot be publicly accessed unless readers make reasonable requests. The data that support the findings of this study are available upon reasonable request from the authors.

CRediT authorship contribution statement

Defeng Wu: Conceptualization, Methodology, Formal analysis, Investigation, Data curation, Writing—Original draft, Visualization. Ting Tang: Conceptualization, Methodology, Supervision, Writing—review & editing. Daniel Odermatt: Conceptualization, Methodology, Supervision, Writing—review & editing. Wenfeng Liu: Conceptualization, Methodology, Resources, Supervision, Project administration, Funding acquisition, Writing—review & editing.

Declaration of competing interest

The authors declare that they have no known competing financial interests or personal relationships that could have appeared to influence the work reported in this paper.

Data availability

The water quality data of 1015 lakes and reservoirs around the world are available from Copernicus Global Land Service (CGLS, https://land.copernicus.eu/global/products/lwq/). The ERA5-Land data are available from the Copernicus Climate Change Service's Climate Data Store (https://cds.climate.copernicus.eu/cdsapp#!/search?type=dataset). The geographic attributes, such as location and area of the catchments, the average depth and discharge, comes from HydroLAKES (Messager *et al* 2016) and Global Lakes and Wetlands Database (GLWD) (Lehner and Döll, 2004). Population distribution data in the year 2020 are available from the Gridded Population of the World (GPW) version 4 of Center for International Earth Science Information Network (CIESIN, https://doi.org/10.7927/H45Q4T5F).

Code availability

R 4.1.2 are used to create all figures and other analysis of this study. The codes are available from the corresponding author upon reasonable request.

ORCID iDs

Defeng Wu https://orcid.org/0009-0005-5687-9610
Ting Tang https://orcid.org/0000-0002-2867-9241
Daniel Odermatt https://orcid.org/0000-0001-8449-0593
Wenfeng Liu https://orcid.org/0000-0002-8699-3677

References

[1] World Meteorological Organization (WMO) 2023, January 12 Past eight years confirmed to be the eight warmest on record. World Meteorological Organization. https://wmo.int/media/news/past-eight-years-confirmed-be-eight-warmest-record
[2] Grant L *et al* 2021 Attribution of global lake systems change to anthropogenic forcing *Nat. Geosci.* **14** 849–54
[3] Woolway R I *et al* 2020 Global lake responses to climate change *Nat. Rev. Earth Environ.* **1** 388–403
[4] Woolway R I *et al* 2021 Lake heatwaves under climate change *Nature* **589** 402–7
[5] O'Reilly C M *et al* 2015 Rapid and highly variable warming of lake surface waters around the globe *Geophys. Res. Lett.* **42** 773–10
[6] Maberly S C *et al* 2020 Global lake thermal regions shift under climate change *Nat. Commun.* **11** 1232
[7] Yao F *et al* 2023 Satellites reveal widespread decline in global lake water storage *Science* **380** 743–9
[8] Li Y, Zhao G, Allen G H and Gao H 2023 Diminishing storage returns of reservoir construction *Nat. Commun.* **14** 3203
[9] Hou X *et al* 2017 Fifteen-year monitoring of the turbidity dynamics in large lakes and reservoirs in the middle and lower basin of the Yangtze River, China *Remote Sens. Environ.* **190** 107–21
[10] Huang J *et al* 2019 How successful are the restoration efforts of China's lakes and reservoirs? *Environ. Int.* **123** 96–103
[11] Vörösmarty C J *et al* 2010 Global threats to human water security and river biodiversity *Nature* **467** 555–61
[12] Hasler A D A 1958 *Treatise on Limnology. vol. I. Geography, Physics and Chemistry. George Evelyn Hutchinson.* (Wiley) 1957. xiv + 1015 pp. Illus. $19. *Science* 127, 88–88
[13] Carpenter D J and Carpenter S M 1983 Modeling inland water quality using Landsat data *Remote Sens. Environ.* **13** 345–52
[14] Zhang L *et al* 2022 Turbidity dynamics of large lakes and reservoirs in northeastern China in response to natural factors and human activities *J. Clean. Prod.* **368** 133148
[15] International Organization for Standardization 2016 ISO 7027-1: Water quality—Determination of turbidity—Part 1: Quantitative methods. ISO. https://iso.org/standard/53639.html
[16] Zhang Y *et al* 2014 Thermal structure and response to long-term climatic changes in Lake Qiandaohu, a deep subtropical reservoir in China *Limnol. Oceanogr.* **59** 1193–202
[17] Qin B *et al* 2020 Water depth underpins the relative roles and fates of nitrogen and phosphorus in lakes *Environ. Sci. Technol.* **54** 3191–8
[18] Jane S F *et al* 2021 Widespread deoxygenation of temperate lakes *Nature* **594** 66–70
[19] Nechad B, Ruddick K G and Park Y 2010 Calibration and validation of a generic multisensor algorithm for mapping of total suspended matter in turbid waters *Remote Sens. Environ.* **114** 854–66
[20] Nechad B, Dogliotti A I, Ruddick K G and Doxaran D Particulate backscattering and suspended matter concentration retrieval from remote-sensed turbidity in various coastal and riverine turbid waters *Submitt. Proc. ESA Living Planet Symp. Prague 9–13 May, ESA-SP 740 (2016)*
[21] Pfannkuche J and Schmidt A 2003 Determination of suspended particulate matter concentration from turbidity measurements: particle size effects and calibration procedures *Hydrol. Process.* **17** 1951–63
[22] Liu D *et al* 2020 Observations of water transparency in China's lakes from space *Int. J. Appl. Earth Obs. Geoinformation* **92** 102187
[23] WHO 2017 Guidelines for drinking-water quality *Incorporating the 1st Addendum.* 4th ed (Geneva: World Health Organization) https://who.int/publications/i/item/9789241549950
[24] Braga F, Scarpa G M, Brando V E, Manfè G and Zaggia L 2020 COVID-19 lockdown measures reveal human impact on water transparency in the Venice Lagoon *Sci. Total Environ.* **736** 139612
[25] Lisi P J and Hein C L 2019 Eutrophication drives divergent water clarity responses to decadal variation in lake level *Limnol. Oceanogr.* **64** S49–59
[26] Deutsch E S, Fortin M-J and Cardille J A 2022 Assessing the current water clarity status of ∼100,000 lakes across southern Canada: a remote sensing approach *Sci. Total Environ.* **826** 153971
[27] Cao Z, Duan H, Feng L, Ma R and Xue K 2017 Climate- and human-induced changes in suspended particulate matter over Lake Hongze on short and long timescales *Remote Sens. Environ.* **192** 98–113
[28] Shi K, Zhang Y, Zhu G, Qin B and Pan D 2018 Deteriorating water clarity in shallow waters: evidence from long term MODIS and *in situ* observations *Int. J. Appl. Earth Obs. Geoinformation* **68** 287–97
[29] Cao Z *et al* 2023 MODIS observations reveal decrease in lake suspended particulate matter across China over the past two decades *Remote Sens. Environ.* **295** 113724
[30] Wang S *et al* 2020 Changes of water clarity in large lakes and reservoirs across China observed from long-term MODIS *Remote Sens. Environ.* **247** 111949
[31] Olmanson L G, Brezonik P L and Bauer M E 2014 Geospatial and temporal analysis of a 20-year record of landsat-based water clarity in Minnesota's 10,000 lakes *JAWRA J. Am. Water Resour. Assoc.* **50** 748–61
[32] Du Y *et al* 2020 Quantifying total suspended matter (TSM) in waters using Landsat images during 1984–2018 across the Songnen Plain, Northeast China *J. Environ. Manage.* **262** 110334
[33] Zeng F *et al* 2023 Monitoring inland water via sentinel satellite constellation: a review and perspective *ISPRS J. Photogramm. Remote Sens.* **204** 340–61
[34] He Y *et al* 2022 Water clarity mapping of global lakes using a novel hybrid deep-learning-based recurrent model with Landsat OLI images *Water Res.* **215** 118241
[35] Shen M *et al* 2020 Sentinel-3 OLCI observations of water clarity in large lakes in eastern China: implications for SDG 6.3.2 evaluation *Remote Sens. Environ.* **247** 111950
[36] Xue K *et al* 2020 Variations of suspended particulate concentration and composition in Chinese lakes observed from Sentinel-3A OLCI images *Sci. Total Environ.* **721** 137774
[37] Stefanidis K, Varlas G, Papaioannou G, Papadopoulos A and Dimitriou E 2023 Assessing temporal variability of lake turbidity and trophic state of European lakes using open data repositories *Sci. Total Environ.* **857** 159618

[38] Zou T et al 2024 Analysis of the temporal and spatial evolution of turbidity in tonle sap lake and its influencing factors Sci. Total Environ. 943 173618
[39] Kendall M G 1975 Rank Correlation Methods (Griffin)
[40] Mann H B 1945 Nonparametric tests against trend Econometrica 13 245–59
[41] Yue S, Pilon P and Cavadias G 2002 Power of the mann–kendall and spearman's rho tests for detecting monotonic trends in hydrological series J. Hydrol. 259 254–71
[42] Sen P K 1968 Estimates of the regression coefficient based on kendall's tau J. Am. Stat. Assoc. 63 1379–89
[43] Simis S, Stelzer K, Müller D and Selmes N 2020 Algorithm theoretical basis document – Lake Water Quality 300m - 1km version 1.0, Copernicus Global Land Operations. https://land.copernicus.eu/en/technical-library/lake-water-quality-v1.0/@@download/file
[44] Binding C E, Jerome J H, Bukata R P and Booty W G 2010 Suspended particulate matter in lake erie derived from MODIS aquatic colour imagery Int. J. Remote Sens. 31 5239–55
[45] Vantrepotte V et al 2011 Seasonal and inter-annual (2002-2010) variability of the suspended particulate matter as retrieved from satellite ocean color sensor over the French Guiana coastal waters J. Coast. Res. 1750 1754
[46] Zhang Y, Shi K, Liu X, Zhou Y and Qin B 2014 Lake topography and wind waves determining seasonal-spatial dynamics of total suspended matter in Turbid Lake Taihu, China: assessment using long-term high-resolution MERIS data PLoS One 9 e98055
[47] Spyrakos E et al 2018 Optical types of inland and coastal waters Limnol. Oceanogr. 63 846–70
[48] Gilarranz L J, Narwani A, Odermatt D, Siber R and Dakos V 2022 Regime shifts, trends, and variability of lake productivity at a global scale Proc. Natl. Acad. Sci. 119 e2116413119
[49] Odermatt D, Danne O, Philipson P and Brockmann C 2018 Diversity II water quality parameters from ENVISAT (2002–2012): a new global information source for lakes Earth Syst. Sci. Data 10 1527–49
[50] Simis S et al 2022 D4.1: Product validation and intercomparison report. https://climate.esa.int/media/documents/CCI-LAKES-0031-PVIR_v2.1.pdf
[51] Stelzer K, Müller D, Simis S and Selmes N 2020 Quality assessment report – Lake Water Quality 300m - 1km version 1.0, Copernicus Global Land Operations. https://land.copernicus.eu/en/technical-library/lake-water-quality-v1.0/@@download/file
[52] Wang S et al 2021 A dataset of remote-sensed forel-Ule index for global inland waters during 2000–2018 Sci. Data 8 26
[53] Zuhlke M, Fomferra N, Brockmann C, Peters M, Veci L, Malik J, Regner P et al 2015 SNAP (Sentinel Application Platform) and the ESA Sentinel 3 Toolbox. In Sentinel-3 for Science Workshop, ESA Special Publication (Vol. 734, pp. 21). European Space Agency. Available at: https://ui.adsabs.harvard.edu/abs/2015ESASP.734E..21Z.
[54] Lehner B and Grill G 2013 Global river hydrography and network routing: baseline data and new approaches to study the world's large river systems Hydrol. Process. 27
[55] Linke S et al 2019 Global hydro-environmental sub-basin and river reach characteristics at high spatial resolution Sci. Data 6 283
[56] Lehner B and Döll P 2004 Development and validation of a global database of lakes, reservoirs and wetlands J. Hydrol. 296 1–22
[57] Muñoz-Sabater J et al 2021 ERA5-Land: a state-of-the-art global reanalysis dataset for land applications Earth Syst. Sci. Data 13 4349–83
[58] Center for International Earth Science Information Network-CIESIN-Columbia University 2018 Gridded Population of the World, Version 4 (GPWv4): Population Count, Revision 11 (Version 4.11) [Data set]. Palisades, NY: NASA Socioeconomic Data and Applications Center (SEDAC). https://doi.org/10.7927/H4JW8BX5
[59] Kummu M, Taka M and Guillaume J H A 2018 Gridded global datasets for gross domestic product and human development index over 1990–2015 Sci. Data 5 180004
[60] Beck H E et al 2023 High-resolution (1 km) Köppen-Geiger maps for 1901–2099 based on constrained CMIP6 projections Sci. Data 10 724
[61] Dong W, Zhang Y, Zhang L, Ma W and Luo L 2023 What will the water quality of the Yangtze River be in the future? Sci. Total Environ. 857 159714
[62] He H, Gao S, Jin T, Sato S and Zhang X 2021 A seasonal-trend decomposition-based dendritic neuron model for financial time series prediction Appl. Soft Comput. 108 107488
[63] Tong Y et al 2017 Decline in Chinese lake phosphorus concentration accompanied by shift in sources since 2006 Nat. Geosci. 10 507–11
[64] Tao S et al 2015 Rapid loss of lakes on the Mongolian Plateau Proc. Natl. Acad. Sci. 112 2281–6
[65] Liu W et al 2020 Global phosphorus losses from croplands under future precipitation scenarios Environ. Sci. Technol. 54 14761–71
[66] Harrison X A et al 2018 A brief introduction to mixed effects modelling and multi-model inference in ecology PeerJ 6 1–32
[67] Hao J and Liu F 2024 Improving long-term multivariate time series forecasting with a seasonal-trend decomposition-based 2-dimensional temporal convolution dense network Sci. Rep. 14 1689
[68] Zhao K et al 2019 Detecting change-point, trend, and seasonality in satellite time series data to track abrupt changes and nonlinear dynamics: A Bayesian ensemble algorithm Remote Sens. Environ. 232 111181
[69] Akbas A 2024 Human or climate? differentiating the anthropogenic and climatic drivers of lake storage changes on spatial perspective via remote sensing data Sci. Total Environ. 912 168982
[70] GEOARC 2021 Ecological and Environmental Status of Global Typical Lakes, National Remote Sensing Center of China, Beijing, China. https://doi.org/10.11878/rp.202110.001137.en, available at: https://chinageoss.cn/knowledgehub/report/reportDetail/63a47d46f64eb66545fa02a0
[71] Liu C et al 2021 The increasing water clarity of Tibetan lakes over last 20 years according to MODIS data Remote Sens. Environ. 253 112199
[72] Bonansea M, Rodriguez M C, Pinotti L and Ferrero S 2015 Using multi-temporal landsat imagery and linear mixed models for assessing water quality parameters in Río Tercero reservoir (Argentina) Remote Sens. Environ. 158 28–41
[73] Hou X et al 2022 Global mapping reveals increase in lacustrine algal blooms over the past decade Nat. Geosci. 15 130–4
[74] Rose K C, Greb S R, Diebel M and Turner M G 2017 Annual precipitation regulates spatial and temporal drivers of lake water clarity Ecol. Appl. 27 632–43
[75] Roulet N and Moore T R 2006 Browning the waters Nature 444 283–4
[76] Mi H, Fagherazzi S, Qiao G, Hong Y and Fichot C G 2019 Climate change leads to a doubling of turbidity in a rapidly expanding Tibetan lake Sci. Total Environ. 688 952–9
[77] Abudu S et al 2016 Integration of aspect and slope in snowmelt runoff modeling in a mountain watershed Water Sci. Eng. 9 265–73
[78] Lana-Renault N, Alvera B and García-Ruiz J M 2011 Runoff and sediment transport during the snowmelt period in a mediterranean high-mountain catchment Arct. Antarct. Alp. Res. 43 213–22
[79] Abd Ellah R G and Sparavigna A C 2023 Combining bathymetric measurements, RS, and GIS technologies for monitoring the inland water basins: a case study of Toshka Lakes, Egypt Egypt. J. Aquat. Res. 49 1–8

[80] Ji G and Havens K 2019 Periods of extreme shallow depth hinder but do not stop long-term improvements of water quality in Lake Apopka, Florida (USA) *Water* **11** https://www.mdpi.com/about/announcements/784
[81] Grossman G M and Krueger A B 1995 Economic growth and the environment* *Q. J. Econ.* **110** 353–77
[82] Hunjra A I, Bouri E, Azam M, Azam R I and Dai J 2024 Economic growth and environmental sustainability in developing economies *Res. Int. Bus. Finance* **70** 102341
[83] Wang W *et al* 2023 A record-breaking extreme heat event caused unprecedented warming of lakes in China *Sci. Bull.* **68** 578–82
[84] Sultonov Z and Pant H K 2023 Potential impacts of climate change on water management in the aral Sea Basin *Water Resour. Manag.* **37** 5743–57